*Mineralogical Magazine* (2020), **84**, 420–434
doi:10.1180/mgm.2020.26

CAMBRIDGE UNIVERSITY PRESS

**Article**

# *In situ* remediation of arsenic-rich mine tailings using slag zero valence iron

Tingting Yue[1,2], Shu Chen[2] and Jing Liu[1]*

[1]School of Resources and Environment, Southwest University, Chongqing 400715 China; and [2]The Key Laboratory of Solid Waste Treatment and Resource, Ministry of Education, Southwest University of Science and Technology, Mianyang 621010 China

**Abstract**

Arsenopyrite (FeAsS) and realgar ($As_4S_4$) are two common arsenic minerals that often cause serious environmental issues. Centralised treatment of arsenic-containing tailings can reduce land occupation and save management costs. The current work examined the remediation schemes of tailings from Hunan Province, China, where by different tailings containing arsenopyrite and realgar were blended with exogenous slag zero valence iron (ZVI). Introducing Fe-oxidising bacteria (*Acidithiobacillus ferrooxidans*) recreates a biologically oxidative environment. All bioleaching experiments were done over three stages, each for 7 days and the solid phase of all tests was characterised by scanning electron microscopy, X-ray diffraction, Fourier-transform infrared spectroscopy, X-ray photoelectron spectroscopy and selective extraction analyses. The results showed that the mixture group reduced arsenic release by 72.9–74.7% compared with the control group. The addition of 0.2 g ZVI clearly decreased arsenic release, and the addition of 4.0 g ZVI led to the lowest arsenic release among all tests. The decrease of arsenic released from the tailings was due to the adsorption and uptake of arsenic by secondary iron-containing minerals and Fe–As(V) secondary mineralisation. The addition of large amounts of ZVI reduced the arsenic detected in the amorphous Fe precipitates. Therefore, a low cost and integrated strategy to reduce arsenic release from tailings is to mix two typical tailings and apply exogenous slag ZVI, which can apply to the *in situ* remediation of two kinds or more arsenic-containing tailings.

**Keywords:** arsenic release, realgar, arsenopyrite, zero valence iron, Shimen mine area, tailings

(Received 9 November 2019; accepted 1 April 2020; Accepted Manuscript published online: 27 April 2020; Associate Editor: Runliang Zhu)

## Introduction

Arsenic in mine waste is a major source of pollution for both surface water and groundwater (Gruyter, 2014; Hudson-Edwards, 2016). Arsenic-containing water causes various health problems, including cancer, skin lesions, cardiovascular diseases and adverse pregnancy outcomes (Henke, 2009; Bowell *et al.*, 2014). Arsenic contamination from historic mine areas has been reported throughout the world, including China (Hui *et al.*, 2002; Rodríguez-Lado *et al.*, 2013; Tang *et al.*, 2016), USA (Goossens *et al.*, 2015), Canada (Van Den Berghe *et al.*, 2018), UK (Smedley *et al.*, 2002; Šlejkovec *et al.*, 2010) among others (Chowdhury *et al.*, 1997; Shrestha *et al.*, 2003; Drahota *et al.*, 2011). In some areas, the concentration of arsenic in groundwater or surface water was found to reach up to $4.8\times10^4$ μg/L (Smedley *et al.*, 2002).

Arsenopyrite (FeAsS) and realgar ($As_4S_4$) are primary arsenic minerals commonly found in metallic mines. Arsenopyrite mainly occurs in the tailings of gold mines (Bao, 1991; Xiang *et al.*, 2000), Pb–Zn mines (Lingmei *et al.*, 2009) and tin mines (Pu, 1950). It results in both acid mine drainage and arsenic release (Corkhill and Vaughan, 2009), and affects the soil and water of the mine area. Chang-Li *et al.* (2013) found that the arsenic content of soil in the Sn–Sb mining area of the Hunan Province was 14.95–363.19 mg/kg. As-rich tailings are common in the Hunan Province of China due to their abundance in polymetallic deposits. Arsenopyrite can generate acid within mine waste, just like pyrite ($FeS_2$), *via* the following reaction:

$$4FeAsS + 11O_2 + 6H_2O \rightarrow 4H_3AsO_3 + 4Fe^{2+} + 4SO_4^{2-} \quad (1)$$

In contrast, realgar commonly occurs in low-temperature hydrothermal deposits (Lengke and Tempel, 2003; Zhu *et al.*, 2015; Fan *et al.*, 2018b) often with quartz ($SiO_2$) and calcite/dolomite ($CaCO_3$ and $MgCa(CO_3)_2$) as associated minerals, while orpiment ($As_2S_3$) can also often be found in the surrounding rocks (Gruyter, 2014). Under aerobic surface conditions, realgar is oxidised gradually to produce arsenic and sulfuric acid *via* the pathway:

$$As_4S_4 + 9O_2 + 10H_2O \rightarrow 4H_3AsO_3 + 4H_2SO_4 \quad (2)$$

Lengke and Tempel (2003) evaluated kinetically the acid production in a natural realgar-based mixed-flow experiment, at 25°C and pH 7−9 to give:

$$[H^+]_{prod} = 7.89[H^+]_{initial} + 2.37 \times 10^{-7} \quad (3)$$

where $[H^+]_{prod}$ is acidity released from oxidation, and $[H^+]_{initial}$ is the initial acidity (Lengke and Tempel, 2003). Because of the small amount of realgar (<1%) and large amount of calcium

*Author for correspondence: Jing Liu, Email: Liujing-vip@163.com
**Cite this article:** Yue T., Chen S. and Liu J. (2020) *In situ* remediation of arsenic-rich mine tailings using slag zero valence iron. *Mineralogical Magazine* **84**, 420–434. https://doi.org/10.1180/mgm.2020.26

(>40%), however, the realgar-containing tailings become alkaline (Gruyter, 2014). For example, the Huangshui Creek in Hunan Province, which flows through the realgar tailings area, has a stable pH at 9.01. For this reason, realgar-containing tailings are usually referred to as alkaline tailings whereas arsenopyrite-containing tailings are usually referred to as acidic tailings.

Various technologies have been designed to minimise arsenic release and limit acid production in mine areas, such as blending (Lottermoser, 2007), stabilisation/solidification (Dermatas *et al.*, 2004) and nano-remediation (Gil-Díaz *et al.*, 2019). Blending, i.e. the addition of some materials to tailings, is one effective method for reducing pollution (Lottermoser, 2007). Blending commonly employs inexpensive materials to help neutralise or adsorb pollutants. Some alkaline materials, such as limestone, coal washery wastes, fine-grained tailings, bauxite and organic waste, have been used for acid buffering or as natural adsorbents (Wang and Reardon, 2001; Bertocchi *et al.*, 2006; Lottermoser, 2007; Liu *et al.*, 2013; Lockwood *et al.*, 2014), and are thus referred to as benign waste relative to sulfidic waste.

Recently, nano-sized, zero-valence iron (nZVI) particles and ZVI-biochar have been used for the remediation of As and Cr (Qiao *et al.*, 2017; Vítková *et al.*, 2018; Liu *et al.*, 2019). Baragaño *et al.* (2020) showed that notable results were obtained for nZVI at a dose of 2% (89.5% decrease in As, TCLP test – toxicity characteristic leaching procedure), and no negative effects on soil parameters were detected. Kim *et al.* (2012) revealed that arsenic concentration extracted by TCLP decreased by 52.25% after stabilisation with sodium-dodecyl-sulfate-coated synthesised nZVI at an iron/tailings ratio of 0.34%. Su *et al.* (2016) reported that the immobilisation efficiency of Cr(VI) and $Cr_{total}$ was 100% and 92.9%, respectively, when the soil was treated with 8 g/kg of biochar–nZVI for 15 days. No single technology could be applied in all of the various arsenic pollution conditions. Some arsenic-containing tailings have large volumes and generate large quantities of acid, which make progressive blending with other tailings or the introduction of ZVI more realistic. So, progressive blending with variant tailings and introducing other materials exogenously becomes more realistic.

A realistic proxy of nZVI is slag ZVI grains from the steel industry, often treated as industry waste, because they are strongly corrosive, but produced in large quantity. Compared with synthetic nZVI, slag ZVI is an inexpensive and economical use of industry waste. Liu *et al.* (2010) used iron slag to remove arsenic from water under acidic conditions (pH < 5), and showed that As adsorbed onto the iron slag. Iron dust was used by Liu *et al.* (2013) to treat arsenic-containing acid mine drainage. At present, there are ~29,000 $m^3$ of arsenic-containing tailings in the Shimen realgar mine area in Hunan Province, which need to be remediated. The introduction of exogenous slag ZVI combined with blending technology might be an efficient remediation strategy for *in situ* arsenic-containing tailings.

The present study aimed to remediate the two common kinds of arsenic-containing tailings (realgar and arsenopyrite) in the Hunan Province of China by using slag ZVI as a blending mixture to reduce arsenic release and acid generation.

## Materials and methods

### Sample preparation and characterisation

Realgar and orpiment commonly originate from hypabyssal epithermal deposits in carbonaceous dolomitic carbonate strata (Zhu *et al.*, 2015). Realgar-containing tailings were collected from the historic realgar mine area in Shimen County, Hunan Province, China. The sampling site was located at 29°38′5″N, 111°01′55″E. The realgar-containing tailings were ground and sieved to 40–100 mesh (150–850 μm) to represent local processing. X-ray fluorescence (XRF) analysis showed that the realgar-containing tailings were composed mainly of CaO (59.02 wt.%), MgO (17.09 wt.%), $SO_3$ (10.25 wt.%), $As_2O_3$ (7.82 wt.%), $SiO_2$ (3.53 wt.%) and $Al_2O_3$ (1.11 wt.%). Arsenopyrite particles were handpicked from samples collected in the Chenzhou Pb–Zn mine, Hunan Province, ground by a ball crusher mill (NETZSCH), and sieved to 20–40 mesh (425–850 μm). Analysis by XRF showed that the arsenopyrite was composed mainly of $As_2O_3$ (21.00 wt.%), $SO_3$ (26.83 wt.%), $Fe_2O_3$ (16.20 wt.%), ZnO (14.59 wt.%), MgO (14.29 wt.%), $SiO_2$ (4.42 wt.%), with minor amounts of $Al_2O_3$ (1.55 wt.%), PbO (0.60 wt.%), CaO (0.25 wt.%) and others (0.22 wt.%). The slag ZVI used in the experiments was collected from the Chenzhou Huasheng steel Co., Ltd (Hunan Province, China). It was black in colour and in granular form. The slag ZVI was also ground and sieved to 40–100 mesh (150–850 μm) to represent local processing. Analysis by XRF showed that the slag ZVI was composed mainly of $Fe_2O_3$ (92.10 wt.%), $SiO_2$ (5.44 wt.%), $Al_2O_3$ (1.11 wt.%), $As_2O_3$ (0.06 wt.%) and others (1.29 wt.%). To remove the surface fine particles and impurities, the ZVI grains were washed with ethanol repeatedly in an ultrasonic bath until the supernatant became clear, then dried at 60°C for 24 h. No attempt was made to remove the oxidised surface because the oxidation was local only and further acid washing might have altered the ZVI grains.

### Bacterial strain

*Acidithiobacillus ferrooxidans*, a common Fe-oxidising bacterium in mine areas, can accelerate the oxidation of pyrite ($FeS_2$)-like sulfide minerals, to produce acid mine drainage (Singer and Stumm, 1970; Fan *et al.*, 2018b). In the present study, the authors used *A. ferrooxidans* to model a biological oxidation environment with rapid acceleration of weathering so that the changes in the two mine wastes with or without ZVI could be observed immediately. The bacterial strain *Acidithiobacillus ferrooxidans* SW 02 used here was provided by the Key Laboratory of Solid Waste Treatment and Resource Recycle, Southwest University of Science and Technology, Mianyang, China. Pure cultures of the *A. ferrooxidans* cells were incubated at 30°C in 9K liquid medium as follows (per 1 L): 0.5 g $K_2HPO_4{\cdot}3H_2O$, 0.01 g $Ca(NO_3)_2$, 0.1 g KCl, 0.5 g $MgSO_4{\cdot}7H_2O$, 3 g $(NH_4)_2SO_4$, 44.3 g $FeSO_4{\cdot}7H_2O$, and pH = 2.2 (adjusted with 5 M $H_2SO_4$) (Silverman and Lundgren, 1959). Cells were harvested during the late exponential growth phase (~3 days after inoculation).

### Batch bioleaching experiment

#### Procedure

Five recipes were examined for blending tests based on future treatment possibilities. These are ('Re' = realgar tailings and 'Ar' = arsenopyrite tailings): the mixture group (1 g Re + 1 g Ar, no ZVI), the 0.2 g ZVI group (1 g Re + 1 g Ar + 0.2 g ZVI), the 4.0 g ZVI group (1 g Re + 1 g Ar + 4.0 g ZVI), the Ar-rich group (0.5 g Re + 1 g Ar + 2.0 g ZVI), and the Re-rich group (1 g Re + 0.5 g Ar + 2.0 g ZVI). These formulations represent the simple mixture of two tailings, the introduction of low- and

https://doi.org/10.1180/mgm.2020.26 Published online by Cambridge University Press

high-ZVI, as well as more acidic and more alkaline tailings in the presence of ZVI, respectively. The two control groups included only arsenopyrite tailings (Ar control) and only realgar tailings (Re control), respectively. Abiotic control was not devised as this study adopted *A. ferrooxidans* only to model accelerated weathering. During bioleaching, the solution (100 mL) containing *A. ferrooxidans* was placed in a 250 mL Erlenmeyer flask, the neck of which was sealed by sterile dressing instead of a glass plug to allow exposure of the solution to ambient air and thus help the growth of *A. ferrooxidans*. Each stage of batch experiments was completed by placing the flask in a rotary shaker at 150 rpm and 30°C for 7 days as *A. ferrooxidans* has a lifetime of ~7 days. After each stage, solids were separated from the suspension by vacuum filtration and dried for 24 h at 80°C. The dried solids were ground gently in a mortar with an agate pestle without compaction of particles, then weighed and used in the next stage at a normalised amount. Three stages were run sequentially to investigate the long-term variations of arsenic release and acid generation. All experiments were done in triplicate. Measured values were described as mean ± standard deviation and plotted with error bars ($n = 3$).

### *Aqueous-phase analysis*

During bioleaching, an aliquot (2 mL) was sampled daily from the supernatant in each Erlenmeyer flask, then filtered (0.45 μm), diluted appropriately with ultrapure water (18.25 MΩ) and acidified with 10 vol.% HCl (Guaranteed Reagent). The pH and Eh were measured using a freshly calibrated pH meter (Sartorius PB-21) and a HACH440d meter with a platinum electrode (MTC10103), respectively. The volume of the suspension was unified by adding stock solution to give a constant solid/solution ratio for all analyses. The As (detection limit was 0.080 mg/L) and Fe (detection limit was 0.002 mg/L) concentrations of the solution were then measured by inductively coupled plasma – atomic emission spectrometry (ICP–AES, iCAP6500 Thermo Fisher, USA). These analyses were undertaken in the Analysis and Test Center, Southwest University of Science and Technology, Mianyang, China. The Ca (detection limit was 0.002 mg/L) concentration was also determined by ICP–AES because the realgar tailings had abundant calcium. The concentration of arsenic released from each group was normalised based on the different initial mass and expressed in the form of milligrams of arsenic per gram of mine waste to characterise clearly, variations during all stages. The ferrous iron in the solution was determined by UV at λ = 510 nm after the application of a phenanthroline spectrophotometric reagent (Liu *et al.*, 2017b). The ferric iron in the solution was obtained by subtracting ferrous iron from total iron.

### *Solid-phase characterisation*

All solid samples were collected from individual batch experiments. As the solid colour may be a potential index for describing the variation of minerals in field tailings, the colour of fresh and wet filtered sample cakes was identified by a standard colorimetric card (standard Munsell colour) as a function of time. The bulk elemental compositions of a powder sample were determined by XRF analysis using a PANalytical Axios instrument equipped with a rhodium anode. The X-ray diffraction (XRD) patterns of the solid samples after bioleaching were recorded using an X'Pert Pro (PANalytical, Netherlands) instrument with a Cu*K*α source. Diffraction data were obtained over a 2θ range of 10–90° with a scan time of 10.16 s per step and a step size of 0.03°. The solid phases were identified using the *Jade 6* software (from Materials Data Inc).

Dried solid samples were subjected to *in situ* infrared spectroscopy using an attenuated total reflection Fourier-transform infrared spectrometer (ATR-FTIR, Frontier) with a diamond ATR accessory. The corresponding spectra ranging from 400 to 4000 $cm^{-1}$ were obtained by co-addition of 64 scans with a resolution of 1 $cm^{-1}$ and a mirror velocity of 0.6329 cm/s. To demonstrate clearly the main variations from arsenic and other molecular vibrations, only the partial spectra in 400–1600 $cm^{-1}$ are shown. The surface morphology and the secondary minerals of raw and leached samples were imaged by scanning electron microscopy (SEM, EVO@18, ZEISS, Germany) equipped with energy-dispersive-X-ray spectroscopy (EDX) operating at 15 kV. The changes in the oxidation state of solid-phase As, Fe and S were determined by X-ray photoelectron spectroscopy (XPS, R3000, VG-Scienta) using an Al*K*α source at 30 eV with a step size of 0.05 eV. The specimen surface was analysed under an argon plasma beam in the vacuum chamber. Photoelectron binding energies were referenced to the C1s level at 284.8 eV. The XPS spectra were obtained at the University of Science and Technology of China, Hefei, China. Deconvolution of the raw data was fitted using *CasaXPS*, and the Shirley-type background was subtracted before deconvolution and fitting (Fan *et al.*, 2018b). The compound peaks of As were determined based on the summary report on arsenopyrite by Corkhill and Vaughan (2009). The binding energies for the component peaks of As, Fe and S were identified by previously reported reference values (Nesbitt and Muir, 1998; Ouyang *et al.*, 2014).

### *Arsenic in amorphous iron precipitates*

Shelobolina *et al.* (1999) investigated the biological dissolution of kaolin by mixed iron-reducing bacteria, and found that the amorphous fraction in solids after leaching was proportional to oxalate-soluble iron. The current study employed the same extraction method to measure the amorphous iron fraction by oxalate dissolution (Shelobolina *et al.*, 1999). Briefly, a dried solid sample (0.5 g) was transferred into a 250 mL flask before the addition of aqueous oxalate (0.02 mol/L, 100 mL and pH = 2.0). The suspension was shaken at 25°C and 150 rpm for 24 h, then passed through 0.45 μm filter and diluted by ultrapure water. The total As and Fe in the solution was analysed by ICP–AES (iCAP6500 Thermo Fisher, USA). All experiments were carried out in triplicate. Figure S1 (Supplementary material – see below) lists the release dynamics of As and Fe (at 0, 0.5, 1, 2, 4, 6, 10, 18 and 24 h) and preliminary investigations showed that for all samples, the arsenic concentration (including iron) in the solution arrived at a plateau within 24 h. The total arsenic in each group was calculated follows: total As in amorphous iron precipitates (mg) = concentration of aqueous As (mg/L) × solution volume (L) × dried weight of initial solids (g)/0.5 g.

## Results and discussion

### *Dynamics of pH and Eh*

The variations of pH and Eh can indicate the dissolution of tailings in the environment (Fan *et al.*, 2018b). Figure 1 shows the

https://doi.org/10.1180/mgm.2020.26 Published online by Cambridge University Press

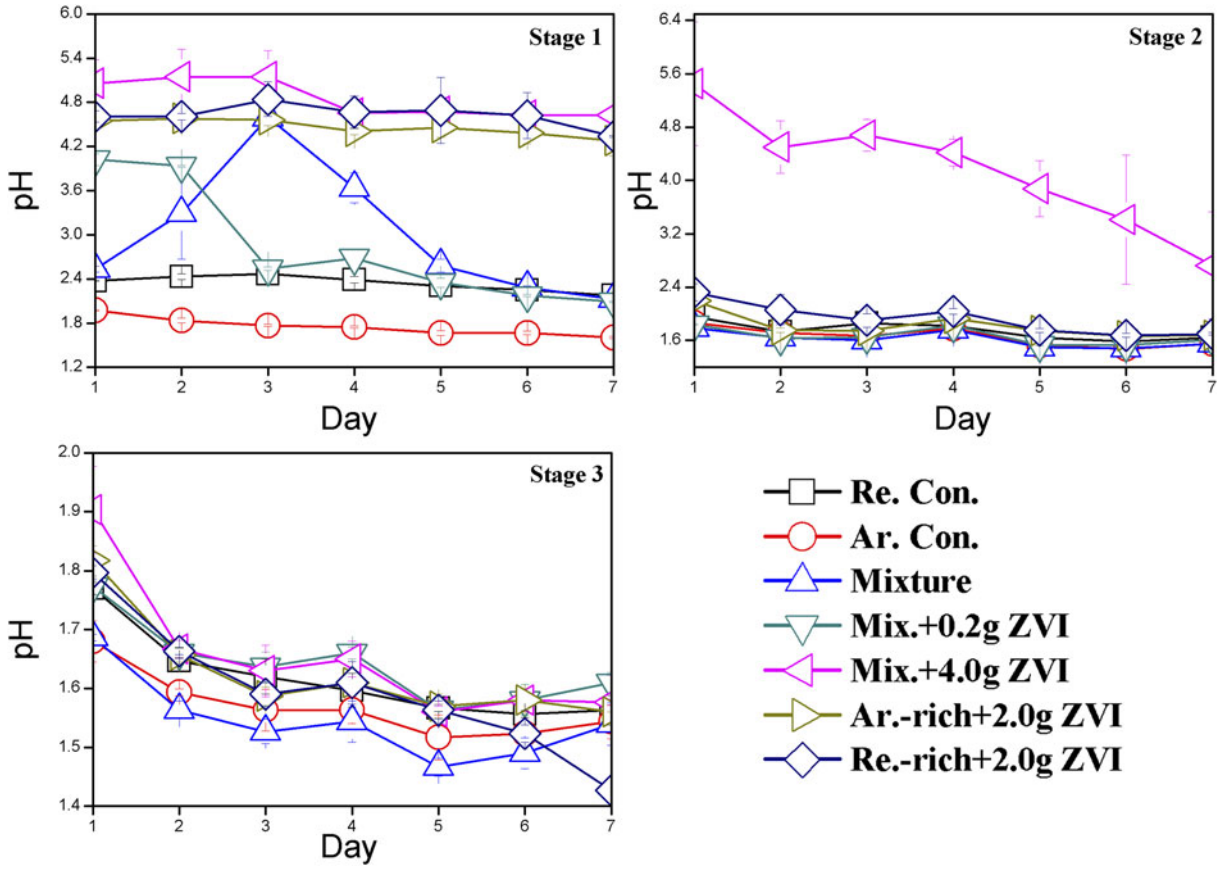


**Fig. 1.** Variation of solution pH over time.

changes in pH as a function of time for the five test groups and the two control groups. In Stage 1, the pH value remained relatively stable at ~2.1–2.4 for the Re control and ~1.9–1.8 for the Ar control, respectively, whereas the pH values of all test groups were higher. For example, the pH of the mixture group increased dramatically to ~4.5 on the third day but then decreased gradually to ~2.4 on the seventh day. In the presence of 0.2 g ZVI, the pH first increased to 4.0 over the first 2 days, and decreased gradually to 2.1 on the seventh day. In contrast, the presence of 4.0 g ZVI kept the pH stable at 4.6–5.0 throughout Stage 1, far exceeding the pH value of all other groups.

The Eh value was the highest in the Re control group, always at ~520–560 mV (Fig. S2). The Eh value of the mixture group remained at ~320 mV over the first 3 days and then increased gradually to ~500 mV on the seventh day. The $Fe^{2+}$ concentration of the mixture group decreased quickly over the first three days (Fig. S3), which resulted in the increase in Eh.

In Stage 2, the pH values of the two control groups were similar and both stayed at 1.6–2.2, whereas the pH of both the mixture group and the 0.2 g ZVI group decreased, to slightly less than the controls. In contrast, the 4.0 g ZVI group still exhibited higher pH, although it declined steadily from 5.5 on the first day to 2.6 on the seventh day. The Eh value of the 4.0 g ZVI group increased from −180 to 210 mV in Stage 2 (Fig. S2), and a quick decrease in $Fe^{2+}$ concentration was also observed (Fig. S3). All groups had pH < 2 in Stage 3. The pH values of the mixture group and the 0.2 g ZVI group still decreased steadily and were both less than the values for the controls. In Stages 1, 2 and 3, only the pH values of the 4.0 g ZVI group and Re-rich group were greater than the control groups. Thus, large amounts of ZVI and more realgar-containing tailings could help maintain higher pH values in the mine waste.

### *Dynamics of As and Fe release*

Levels of arsenic release from all groups over the three stages are shown in Fig. 2. In Stage 1, the arsenic concentration of the Ar control rose dramatically, from 43.89 mg/g on the first day to 105.49 mg/g on the seventh day, whereas the Re control during this Stage released relatively little arsenic to the solution (~0.13 mg/g). By mixing the two tailings, the mixture group showed an arsenic release that was 72.9–74.7% lower than the Ar control, i.e. down to 12.19 mg/g on the first day and 28.01 mg/g on the seventh day.

The arsenic release was clearly curtailed by the addition of ZVI. When 0.2 g ZVI was present, the arsenic release was initially 0.10 mg/g on the first day and gradually increased to just 29.89 mg/g on the seventh day (Fig. 2). Further addition of ZVI to a total of 4.0 g reduced the arsenic release even further, in fact even lower than that of the Re control. The arsenic release fell in the order of Ar-rich group > Re-rich group > 4.0 g ZVI group > Re control group. Note that both the Ar-rich and the Re-rich groups contained 2.0 g ZVI in their formulations.

In Stage 2, the increase in arsenic release of the Ar control became accentuated compared with Stage 1, increasing from a smaller starting value of 24.47 mg/g on the first day to a larger value of 127.44 mg/g on the seventh day. The arsenic release of the mixture group was 52.0–52.7% less than that of the Ar control

https://doi.org/10.1180/mgm.2020.26 Published online by Cambridge University Press

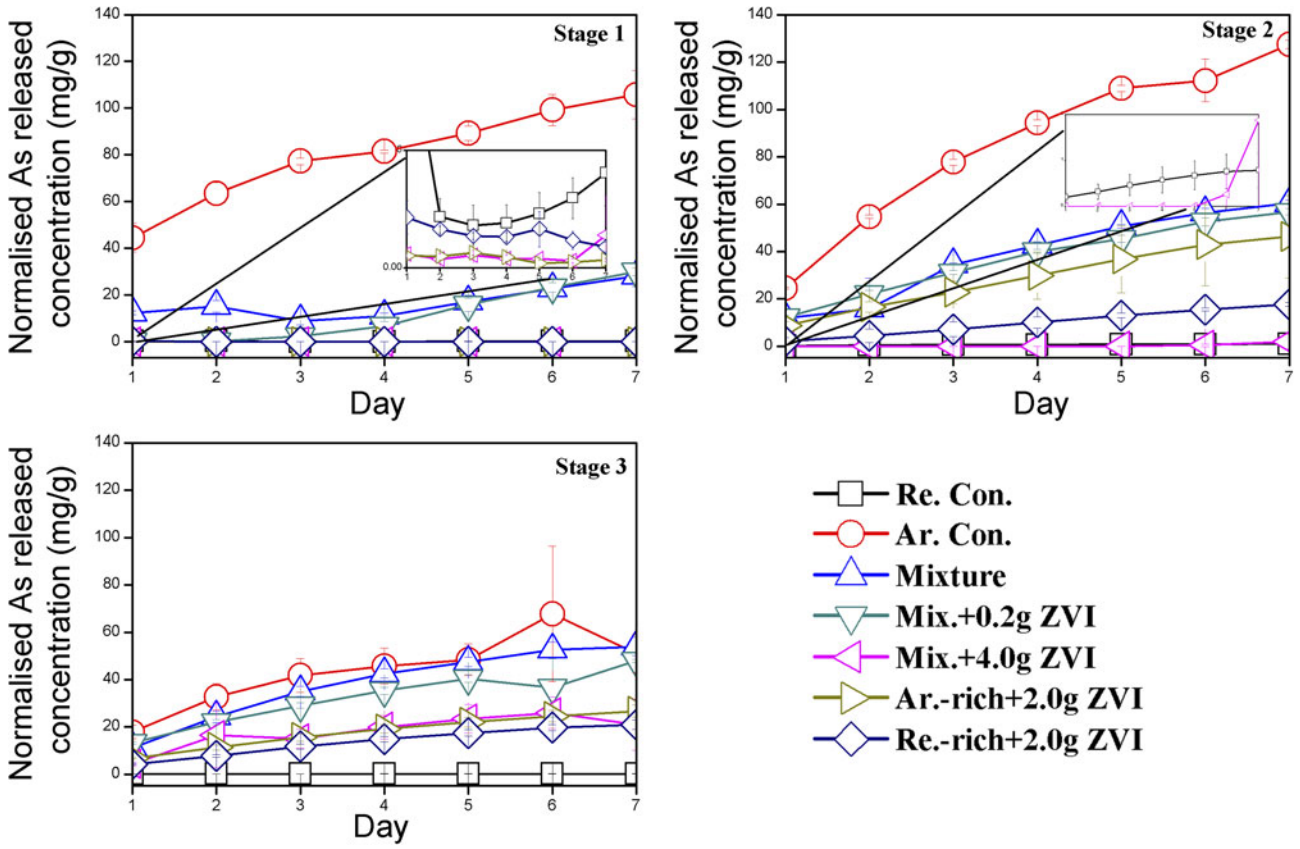


**Fig. 2.** Arsenic release as a function of time.

group and increased to 60.22 mg/g on the seventh day. The arsenic release of the 0.2 g ZVI group was very similar to that of the mixture group. Because variation in the Ar control experiment was accentuated in Stage 2 compared to Stage 1, the difference between the Re-rich and Ar-rich groups, both containing 2.0 g ZVI, should, theoretically, become distinctive from Stage 1. In fact, a larger difference was observed between the Ar-rich group and the Re-rich group, indicating that the strategy of controlling arsenic by regulating the proportions of various tailings is also effective with identical intermediate ZVI addition. Still, the 4.0 g ZVI group exhibited the smallest amount of arsenic release of only 0.0035–1.89 mg/g throughout the entire stage, which was even less than that from the Re control (~0.79 mg/g).

In Stage 3, the absolute value of arsenic release of the Ar control group decreased further, from 17.5 mg/g on the first day to 53.11 mg/g on the seventh day. The arsenic release of the Ar control group was relatively low compared to those in Stages 1 and 2. This suggested that arsenopyrite oxidation occurred to a lesser degree in Stage 3. The precipitation of jarosite was observed (Fig. 4*b*, Fig. S5), which retarded the adsorption of bacteria on the arsenopyrite surface (Henao and Godoy, 2010; Deng *et al.*, 2018). The Re control group exhibited the lowest arsenic release of 0.10–0.18 mg/g throughout Stage 3. That might be related to a reduced level of oxidation of realgar. The mixture group showed a similar pattern but the actual arsenic release was 5.9–37.0% lower than the Ar control. The 0.2 g ZVI group actually showed greater arsenic release than the mixture group, indicating that the utility of the starting 0.2 g ZVI in controlling arsenic release had been exhausted. After proceeding from Stage 2 to Stage 3, the arsenic release of the Ar-rich group declined by ~50%, but that of the Re-rich group remained more or less at the same level. Hence, adjusting the mixing ratio of tailings had an obvious impact on arsenic control in Stage 3. That is, alkali tailings slowed the dissolution of arsenopyrite.

Stage 3 arsenic concentrations were relatively small compared to those in Stage 2, except for the 4.0 g ZVI group. The decrease in arsenic was due to the adsorption and uptake of arsenic by secondary iron-containing minerals and Fe–As oxysalts. The 4.0 g ZVI group actually released more arsenic in Stage 3 than it did during the two previous stages, probably because the arsenic that was adsorbed on the Fe precipitates became liberated, as will soon be demonstrated in the subsequent sections.

## *Formation of secondary phases and arsenic components*

### *Variations in the colours of solid samples*

The colour change of the solids is related to secondary iron minerals (Schwertmann and Cornell, 1993). The different concentrations of $AsO_4^{3-}$ and $AsO_3^{3-}$ in the $SO_4$–Fe(III) system also changes the colour of precipitates (Liu *et al.*, 2014). Pictures of the filter cakes of all groups in all stages are shown in Fig. 3. The Re control group had a darker colour than the Ar control group, varying from strong dark brown (7.5YR/5/8) in Stage 1 to yellowish brown (10YR/5/8) in Stage 2 and then light olive brown (2.5Y/5/8) in Stage 3. The colour of the Ar control group changed from pale yellow (5Y/7/4) in Stage 1 to olive yellow (5Y/6/6) in Stage 2 and then olive (5Y/5/6) in Stage 3. The mixture group showed a similar colour variation to that of the Ar control group. The 0.2 g ZVI group varied from yellowish

https://doi.org/10.1180/mgm.2020.26 Published online by Cambridge University Press

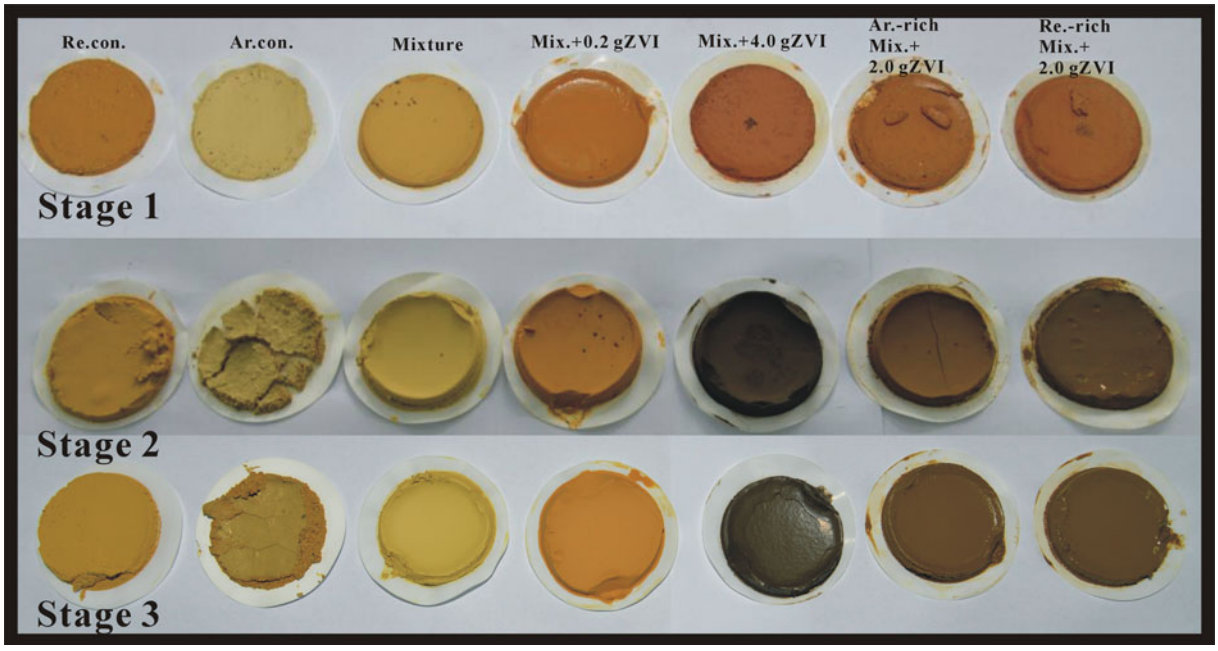


**Fig. 3.** Visible changes in colour during dissolution of tailings by *A. ferrooxidans*.

red (5YR/5/8) in Stages 1 and Stage 2 to reddish yellow (7.5YR/6/10) in Stage 3.

The 4.0 g ZVI group was clearly the darkest among all, having a colour changing from yellowish red (5YR/4/8) during Stage 1 to black (10 YR/2/1) in Stages 2 and 3. The drastic colour change from Stage 1 to Stage 2 matched the sudden surge of the Eh value (−100 mV in Stage 1 to 200 mV in Stage 2). The colour change was similar for the Ar-rich and Re-rich groups and could be associated in both cases with the observed gentle h variation in Eh (Fig. S2). Hence, colour could be used to help to indicate the degree of bioleaching for the mine waste undergoing remediation.

### *Comparison of secondary minerals*

The mineralogical phases of all sample groups are shown in Fig. S5, and Fig. 4 presents SEM images that illustrate the changes of solids morphology under biological dissolution and fresh ZVI. The Re control group exhibited three kinds of jarosite minerals in the solid phase, jarosite $KFe_3(OH)_6(SO_4)_2$, hydroniumjarosite $(H_3O)Fe_3(SO_4)_2(OH)_6$, and ammoniojarosite $(NH_4)Fe_3(OH)_6(SO_4)_2$. In addition, $Ca_3(AsO_4)_2$ was also identified in the tailings. Analysis by XRD indicated that solids from the Ar control only contained jarosite, and no other crystalline components were detected, which was in agreement with the previous observation by Corkhill and Vaughan (2009). The SEM results further showed that three main crystal planes of jarosite developed, i.e. faces (012), (021) and (113) (Fig. 4*b*). The fresh tailings of the Re control had grains with an irregular appearance (Fig. 4*a*). After bioleaching, the crystal planes of grains developed and some grains were cemented (Fig. 4*c*). Fresh ZVI had a granular shape (Fig. 4*d*) but this could not be discerned after bioleaching. In the mixture group, a phase of iron sulfate ($Fe_2(SO4)_3$) was found along with jarosite and dimorphite. In the 0.2 g ZVI group, iron arsenate ($FeAsO_4$) was also observed. It has been reported that scorodite ($FeAsO_4{\cdot}2H_2O$) is a good mineral trap to control arsenic release because of its very low solubility (0.33–5.89 mg/L at pH = 5.01–6.99, $K_{sp} = 10^{-21.66}$ at 22°C) (Langmuir *et al.*, 2006; Bluteau and Demopoulos, 2007). A small amount of schwertmannite ($Fe_8O_8(OH)_6SO_4$) was also observed in the Re-rich group. In addition, some secondary crystalline Fe minerals such as goethite (α-FeOOH), iron oxide hydroxide (FeOOH), lepidocrocite (γ-FeO(OH)) and magnetite ($Fe_3O_4$) were also found. In agreement with the colour changes, in the 4.0 g ZVI group, needle-like precipitates of goethite were observed (Fig. 4*f*). The adsorption capacity of arsenic on goethite (α-FeOOH) is 11.4 mg/g for As(V) at pH = 2 (Mohapatra *et al.*, 2006) and 7.5 mg/g for As(III) at pH = 5.5 (Ladeira and Ciminelli, 2004). The re-adsorption of arsenic on these secondary minerals and mineralisation of Fe–As(V) species is arguably a key mechanism for arsenic removal.

### *FTIR characterisation of the solid phase*

The ATR–FTIR spectra of solids from all groups at all stages is shown in Fig. 5. Solids from the Ar control group clearly had more peaks than those of the Re control group in Stage 1. These peaks occurred at 1203, 1076, 996, 627 and 466 $cm^{-1}$, which originated from the $\nu_3$ (1203 and 1076 $cm^{-1}$), $\nu_1$ (996 $cm^{-1}$), $\nu_4$ (627 $cm^{-1}$) and $\nu_2$ (466 $cm^{-1}$) vibrations of $SO_4^{2-}$, respectively (Liu *et al.*, 2016). The intensities of the peaks increased due to dissolution of tailings and secondary mineralisation. All peaks from the solids of the mixture group had weaker intensity than those of the control groups, indicating that the dissolution of tailings slowed in the mixture group. Solids of the 4.0 g ZVI group showed a weak peak at 743 $cm^{-1}$, which could be attributed to the vibration of As–OH and confirmed the presence of a certain amount of arsenate in the precipitates (Goldberg and Johnston, 2001). Free $AsO_3^{3-}$ in solution has a planar molecular structure (Loehr and Plane, 1968; Tossell, 1997). As there were no obvious $SO_4^{2-}$ peaks in the solids of the 4.0 g ZVI group, which implied crystalline minerals were not abundant, arsenite existed mainly in the form of adsorbed species. The solids of the Re-rich group had more FTIR peaks than those of Ar-rich group, and peaks related to arsenite and arsenate were observed at 745, 792 and 892 $cm^{-1}$. Free $AsO_4^{3-}$ has a tetrahedral structure and gives four vibration modes $\nu_1$, $\nu_2$, $\nu_3$ and $\nu_4$ at 837,

https://doi.org/10.1180/mgm.2020.26 Published online by Cambridge University Press

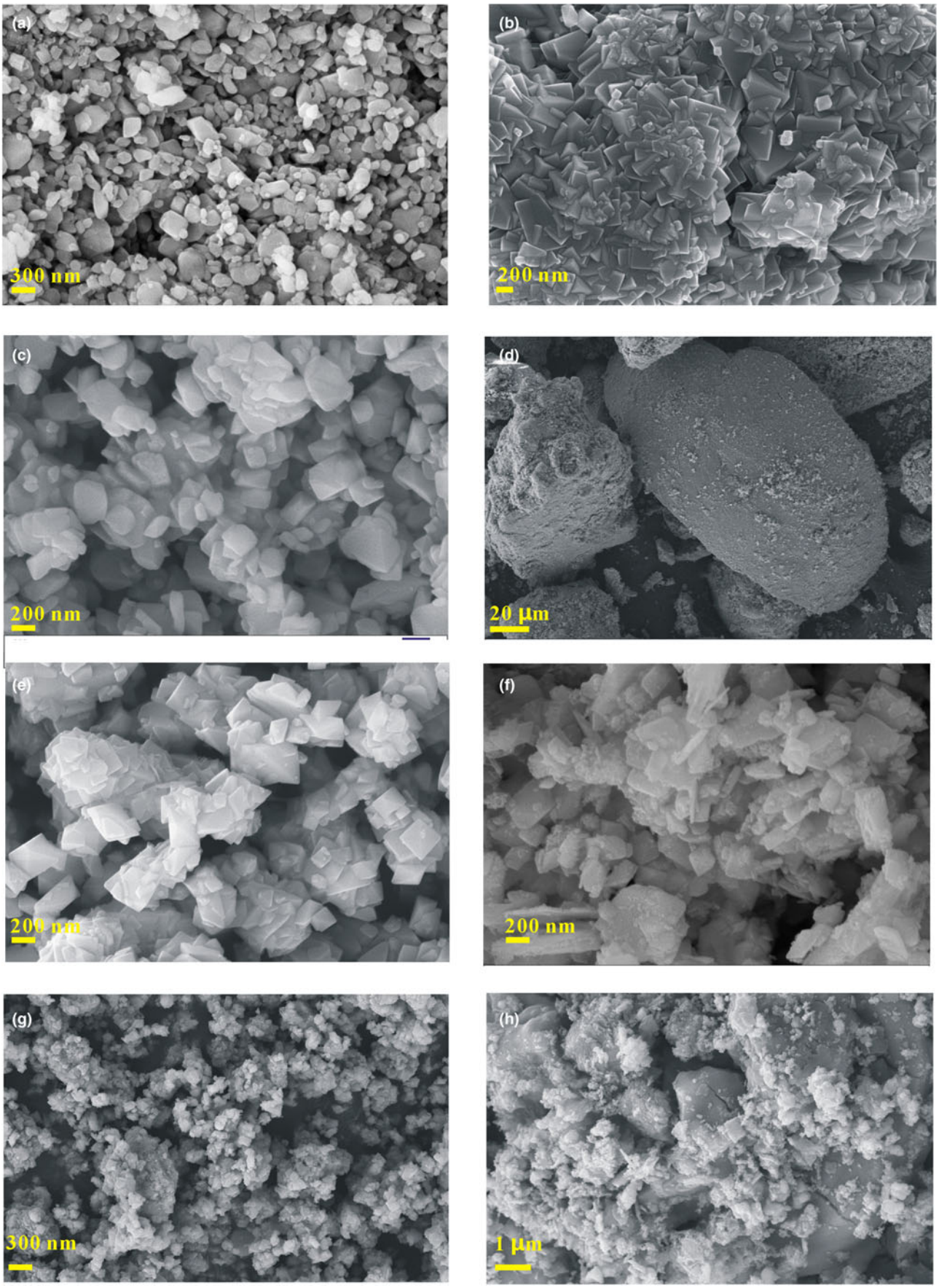


**Fig. 4.** Scanning electron microscope images of various samples under biological dissolution and with ZVI. (*a*) Re control; (*b*) Ar control; (*c*) mixture group; (*d*) fresh ZVI; (*e*) mixture + 0.2 g ZVI group; (*f*) mixture + 4.0 g ZVI group; (*g*) Ar-rich group; and (*h*) Re-rich group.

https://doi.org/10.1180/mgm.2020.26 Published online by Cambridge University Press

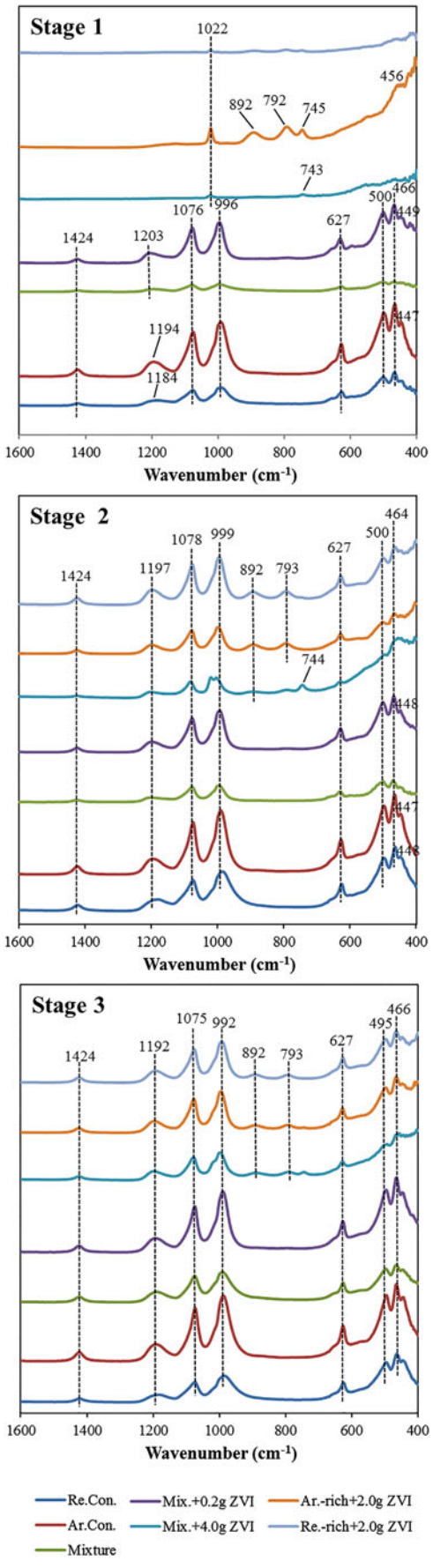


**Fig. 5.** ATR-FTIR spectra of solid products of tailing dissolution experiments.

349, 878 and 463 $cm^{-1}$ (Liu *et al.*, 2017a). The weathering of arsenopyrite and realgar generates arsenite as the dominant species (Fan *et al.*, 2018b), and further oxidation converts dissolved arsenite ($AsO_3^{3-}$) to arsenate ($AsO_4^{3-}$). For the Re-rich group, adsorbed arsenate species showed only a weak peak at 1022 $cm^{-1}$ in the FTIR. Therefore, the Re-rich group appeared to be superior to the Ar-rich group in controlling arsenic release. This was in agreement with the preceding solution analyses, where the Ar-rich group was found to release more arsenic than the Re-rich group.

All FTIR peaks from the solids of all groups intensified in Stage 2 compared with Stage 1, suggesting continuous decomposition of tailings. The greater intensity of the weak peak at 744 $cm^{-1}$ in the solids of 4.0 g ZVI group suggested that more arsenite occurred in the solid phase than in Stage 1. In comparison, a broad peak occurred at 892 $cm^{-1}$ for the solids of the Re-rich and Ar-rich groups, which could also be associated with the presence of arsenite in Stage 2. No characteristic peak of arsenite or arsenate was observed in the solids of the 0.2 g ZVI group. Hence, increasing the amount of ZVI added could assist the formation of amorphous Fe precipitates if the dissolution rate of tailings remained constant. As these precipitates provided more sites to adsorb arsenite and arsenate, the arsenic content in solids also became higher in the 4.0 g ZVI, Re-rich and Ar-rich groups.

All peaks became sharpest in Stage 3. No obvious difference was noted between the solids of the Re-rich and Ar-rich groups. The arsenate peak at 892 $cm^{-1}$ became visible for the solids in the 4.0 g ZVI group, which suggested a greater abundance of arsenate species. The Eh of the 4.0 g ZVI group also jumped from –180 mV in Stage 2 to 480 mV in Stage 3 (Fig. S2). For the mixture group and the ZVI groups, Stage 3 showed no new peaks and the peak intensity increased gradually compared with Stage 2. Peak intensities appeared relatively low for all the ZVI groups. It could be inferred that the addition of ZVI delayed the dissolution of sulfide tailings, but this delay came at the expense of ZVI corrosion. Not also that the solids from the 4.0 g ZVI group always exhibited the lowest $Fe^{3+}$ content compared with others (Fig. S5).

### *Comparison of As valence*

As(III) and As(V) were shown in Fig. 6 to be the dominant valences of As in the collected solids, and Fig. 7 gives the corresponding XPS spectra of the solids collected for all groups in all stages. The Re control group always had less As(III) and As(V) than the Ar control group. It was found previously from the oxidative dissolution of arsenopyrite in the presence of *Leptospirillum ferrooxidans*, a common acid mine drainage bacterium, that arsenic is oxidised more rapidly than S and Fe (Corkhill and Vaughan, 2009). The addition of ZVI clearly reduced the amount of As(III) and As(V) in the precipitates (Fig. 6). The preceding analyses also showed that ZVI reduced the arsenic release into the solution, and it can thus be inferred that ZVI slowed down the oxidation of the tailings, which is an additional line of evidence to support the effect of ZVI in controlling the arsenic pollution of mine waste. With the progression of the oxidation stages, the peak area of various arsenic valence states from each group decreased gradually, especially for the groups with ZVI addition. It could be seen after normalising the surface area that for the precipitates of the Ar control, the total arsenic after three stages was 54.5% As(V), 31.4% As(III) and 14.1% As(I). The addition of ZVI increased the quantity of As(III) in the precipitates from 33.5% to 35.1% and As(I) from 14.1% (for the 0.2 g ZVI group) to 20.3% (for the 4.0 g ZVI

https://doi.org/10.1180/mgm.2020.26 Published online by Cambridge University Press

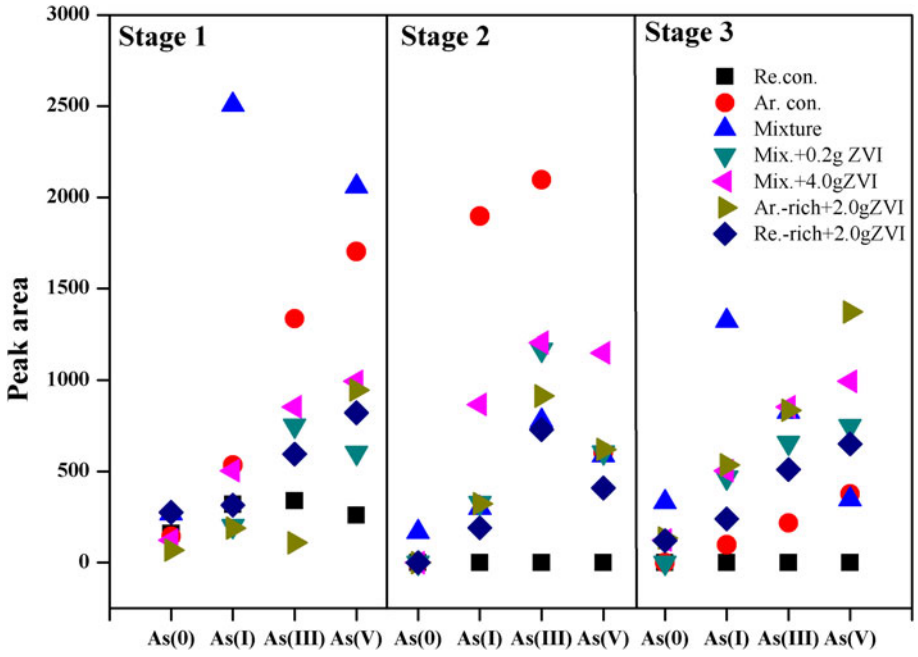


**Fig. 6.** Valences of arsenic in the solid phase.

group). Thus, the oxidation state is related directly to the bioaccessibility of arsenic (Van Den Berghe *et al.*, 2018).

Compared with the Ar control group, the solids of the mixture group obviously had less As(V) (only 12.3%), similar As(III) and higher As(I) (46.8%). In fact, the percentage of As(I) was far greater than the solids of all other groups (14.1–24.9%), even including the Re control group. The greater abundance of intermediate valance states, i.e. As(I) and As(III), and the decrease in As(V) could be attributed to slower oxidation. It could thus be inferred that the mixture group reduced arsenic release not only by re-adsorption and mineralisation but also by passivation.

### *Main mechanisms*

In the Re control group, the $Fe^{2+}$ was oxidised to $Fe^{3+}$ by dissolved $O_2$ or *A. ferrooxidans* (equation 4). The $Fe^{3+}$ can accelerate realgar-containing tailings decomposition. Dissolution of calcium-containing minerals in the Re control group increases the pH of the solution (equation 5).

$$4Fe^{2+} + O_2 + 4H^+ \xrightarrow{A.\ ferrooxidans} 4Fe^{3+} + 2H_2O \quad (4)$$

$$CaMg(CO_3)_2 + 4H^+ \rightarrow Ca^{2+} + Mg^{2+} + CO_2 \uparrow + 2H_2O \quad (5)$$

Both $O_2$ and $Fe^{3+}$ are the main oxidants of arsenopyrite, and acid is produced after the oxidation (equations 6 and 7). Because $Fe^{3+}$ has a greater impact than $O_2$ on the oxidation rate of arsenopyrite (He *et al.*, 2019), lower $Fe^{3+}$ concentration in the solution may help to slow the dissolution of As. In Stage 1, the $Fe^{3+}$ concentration measured in the solution was as low as 1.34–14.87 mg/g for the mixture group, but 165.99–237.41 mg/g for the Ar control and 166.07–48.43 mg/g for the Re control groups (Fig. S4).

$$4FeAsS + 13O_2 + 6H_2O \rightarrow 4FeSO_4 + 4H_3AsO_4 \quad (6)$$

$$FeAsS + 11Fe^{3+} + 7H_2O \rightarrow H_3AsO_3 + 12Fe^{2+} + SO_4^{2-} + 11H^+ \quad (7)$$

The dissolution of slag ZVI also consumes the $H^+$ in the solution produced by the oxidation of the tailings, and then generates hydrogen gas, produces $Fe^{2+}$ and leads to an increase in the solution pH (equation 8). Dissolved *A. ferrooxidans* can oxidise $Fe^{2+}$ to $Fe^{3+}$ (equation 4), which could then result in $Fe^{3+}$ precipitates (equation 9). The precipitation of $Fe^{3+}$ commonly begins at pH = 3.2 (Liu *et al.*, 2013). The transformation of the iron species in the precipitates can be confirmed by the colour changes of the precipitates and by aqueous analysis (Fig. S3).

$$Fe^0 + 2H^+ \rightarrow Fe^{2+} + H_2 \uparrow \quad (8)$$

$$Fe^{3+} + 3OH^- \rightarrow Fe(OH)_3 \downarrow \quad (9)$$

In Stage 2, the concentration of $Fe^{3+}$ in the solution remained stable in the 4.0 g ZVI group at ~4.59–12.39 mg/g, which was the lowest in all other groups. Meanwhile, $Fe^{2+}$ became the dominant species, with a concentration 10 times that of $Fe^{3+}$ (Fig. S3). The addition of ZVI introduced a variety of secondary iron-containing minerals, such as goethite, schwertmannite and lepidocrocite, all of which could adsorb or co-precipitate with As(V) and As(III) (equations 10–12). The $Fe^{2+}$ generated in equation 11 would have been an additional source of $Fe^{2+}$ for *A. ferrooxidans* to generate $Fe^{3+}$, which could in turn form additional $Fe^{3+}$ precipitates.

$$Fe^{3+} + H_3AsO_4 \rightarrow FeAsO_4 \downarrow + 3H^+ \quad (10)$$

$$3Fe^{3+} + K^+ + 2nSO_4^{2-} + (1-2n)AsO_4^{3-} + 6H_2O \rightarrow KFe_3(SO_4)_{2n}(AsO_4)_{(1-2n)}(OH)_6 + 6H^+ \quad (11)$$

$$3Ca^{2+} + 2AsO_4^{3-} \rightarrow Ca_3(AsO_4)_2 \downarrow \quad (12)$$

Rich $Fe^{2+}$ could maintain a relatively reducing environment and assist the oxidation of As(III) (Liu *et al.*, 2019).

https://doi.org/10.1180/mgm.2020.26 Published online by Cambridge University Press

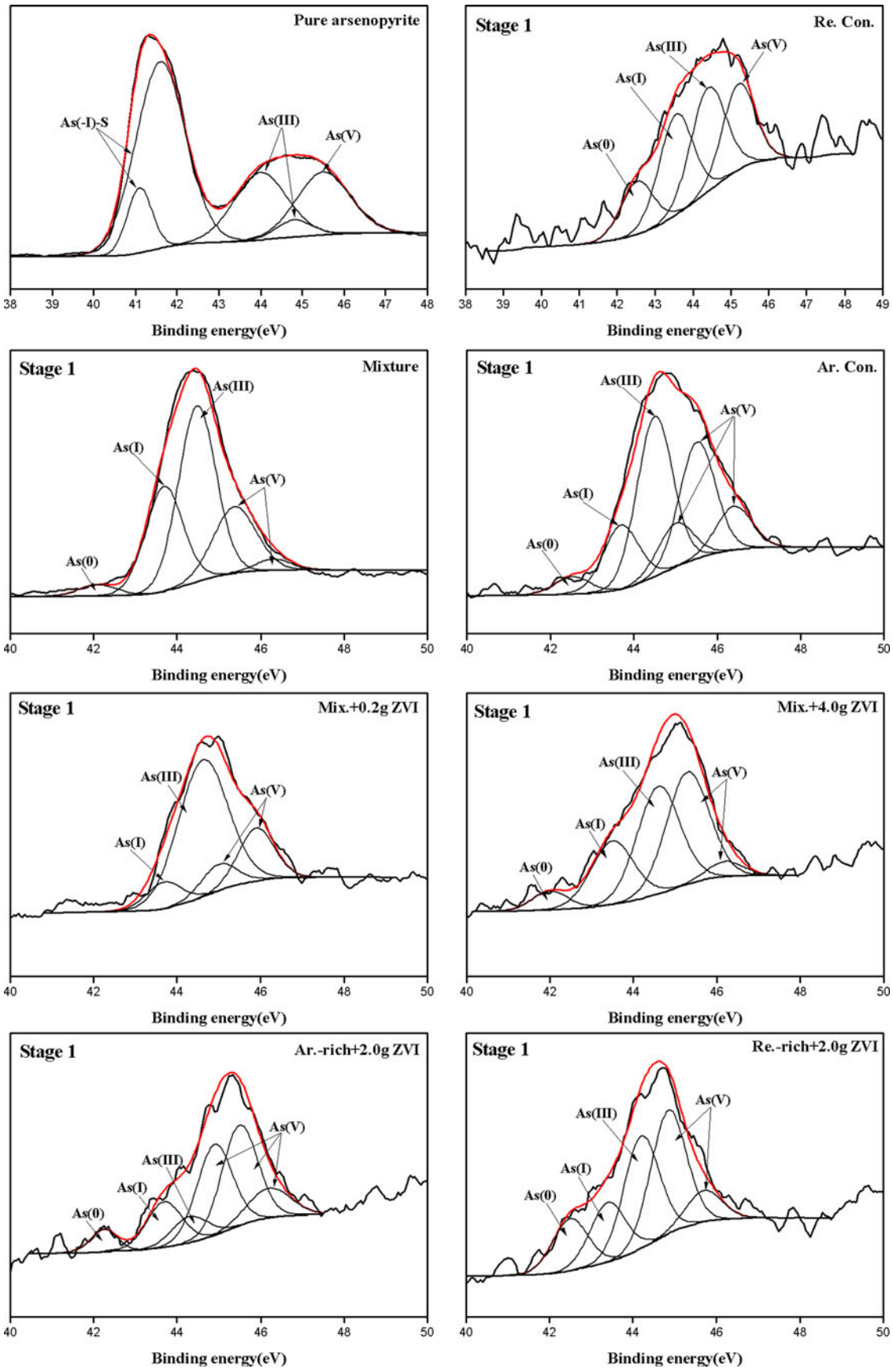


**Fig. 7.** XPS spectra in As 3d regions of solid products after biological dissolution for all groups in all stages.

https://doi.org/10.1180/mgm.2020.26 Published online by Cambridge University Press

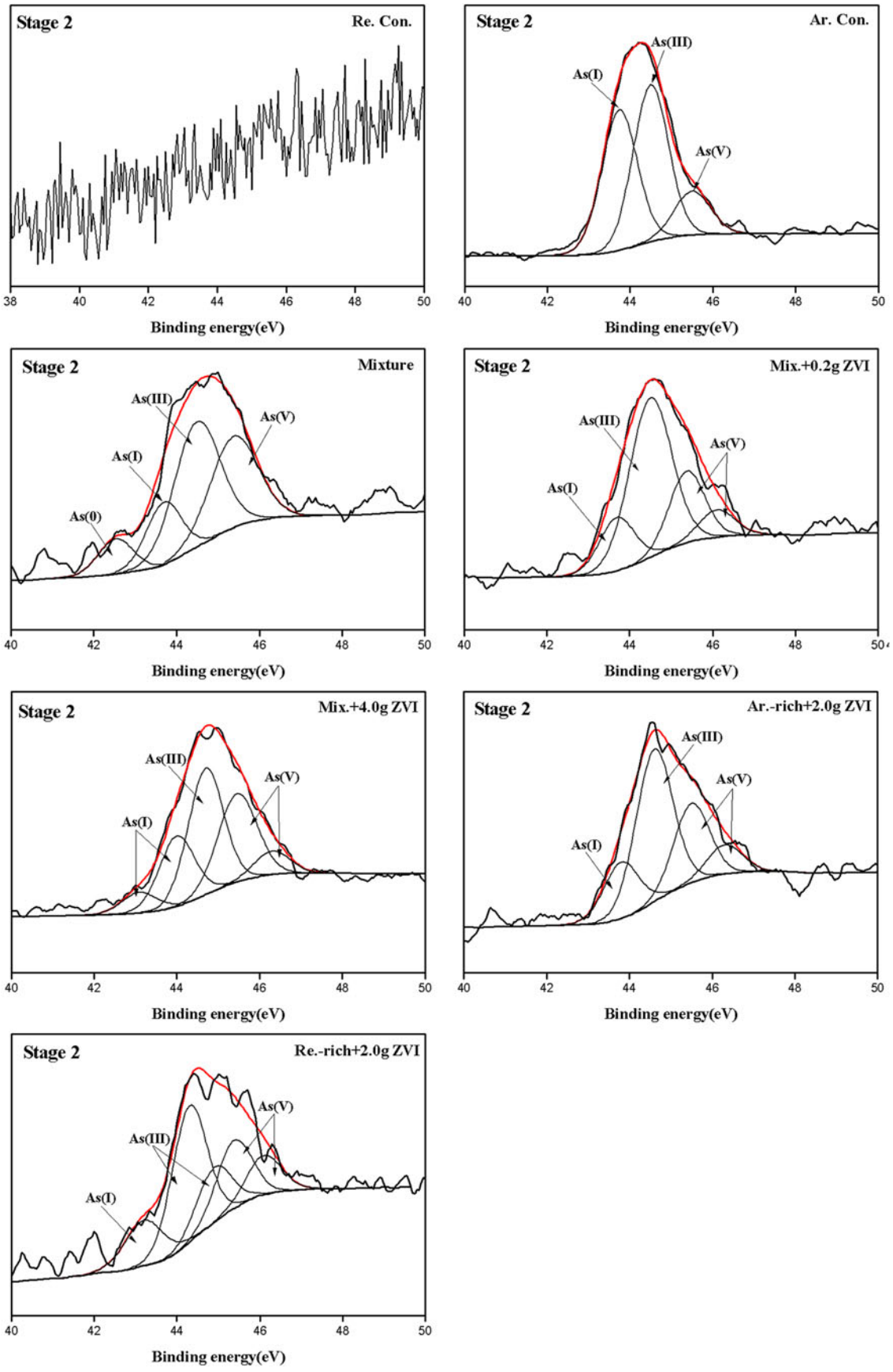


**Fig. 7.** Continued.

https://doi.org/10.1180/mgm.2020.26 Published online by Cambridge University Press

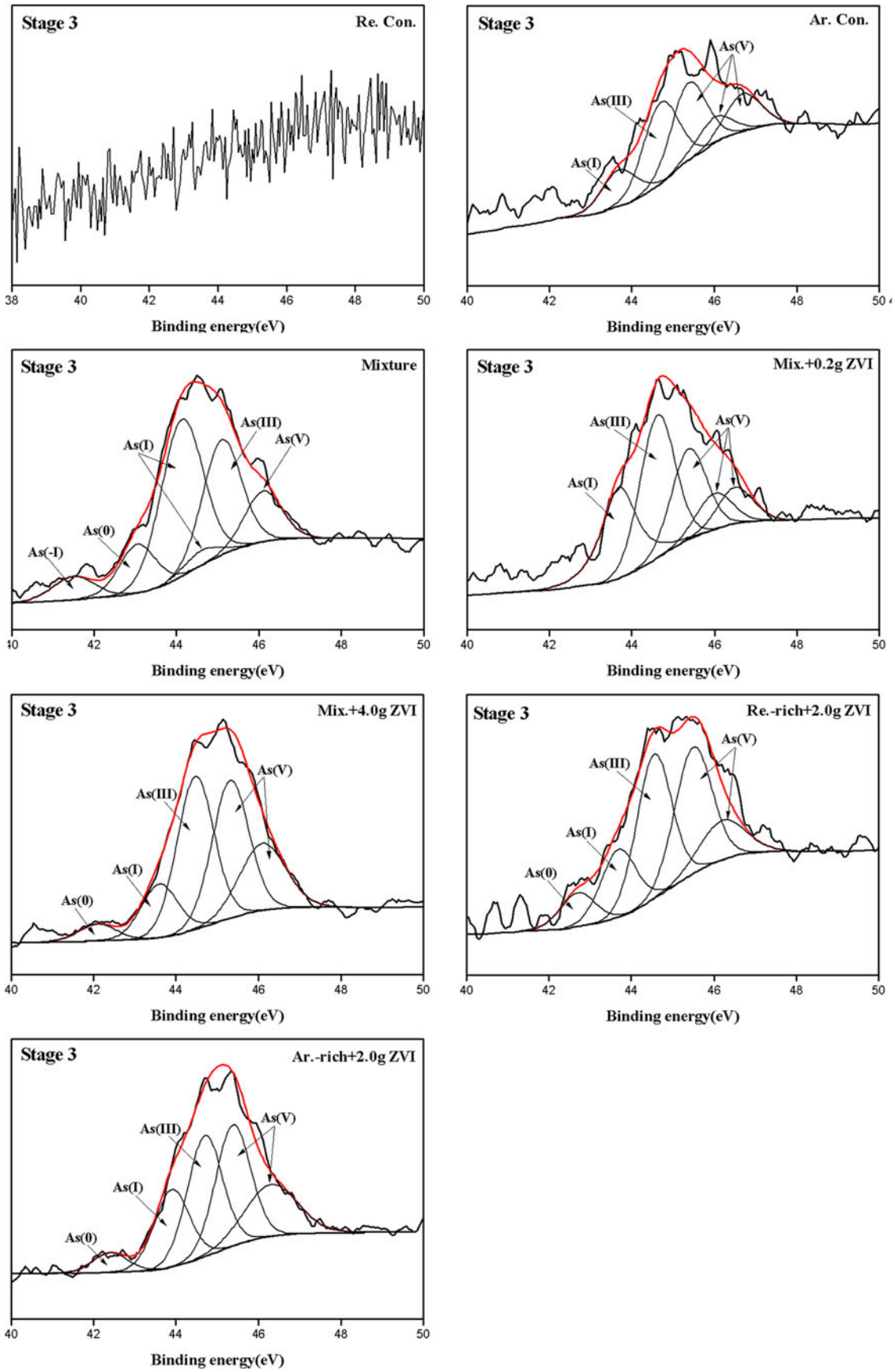


**Fig. 7.** Continued.

https://doi.org/10.1180/mgm.2020.26 Published online by Cambridge University Press

The increased As(III) peak area in Stage 2 of the ZVI experiments indicated that some of the As(V) produced by oxidation of As(III) was reduced to As(III). This probably occurred through reduction of the As(V) by the ZVI, which in turn oxidised, producing additional $Fe^{2+}$. This process, shown in equation 13, would have led to further generation of $Fe^{2+}$, which would, in turn, have oxidised to $Fe^{3+}$ to generate more secondary As–Fe phases.

$$2Fe + H_3AsO_4 + 2H^+ \rightarrow 2Fe^{2+} + H_3AsO_3 + H_2O \quad (13)$$

Carlson *et al.* (2002) found that the schwertmannite they synthesized in the laboratory had an adsorption capacity of as much as 175 mg/g at pH = 3 for As(V). The maximum adsorption capacity of ferrihydrite, also an amorphous Fe-containing mineral, is 19.9 mg/g at pH = 5 for As(III) (Carlson *et al.*, 2002) and 210 mg/g at pH = 3 for As(V) (Teixeira and Ciminelli, 2005). These minerals could thus provide additional As removal by sorption or co-precipitation, as can be seen from ATR–FTIR, XPS and XRD observations.

Crystalline iron arsenate ($FeAsO_4$), which can improve the stability of arsenic in the solid phase, was also found in this study. The chemical extraction of arsenic in amorphous Fe precipitates is shown in Fig. 8. Overall, the amount of arsenic in the precipitates increased gradually in Stage 2 with the progression of oxidation stages for all groups. The amount of arsenic in amorphous Fe precipitates increased in Stage 2, and decreased in Stage 3 for the 0.2 g ZVI group but increased gradually for the 4.0 g ZVI group. In Stage 3, the amount of arsenic in the precipitates of the 4.0 g ZVI group exceeded that of the Ar-rich and Re-rich groups, thus accounting for the slight increase in arsenic release of the 4.0 g ZVI group in Stage 3.

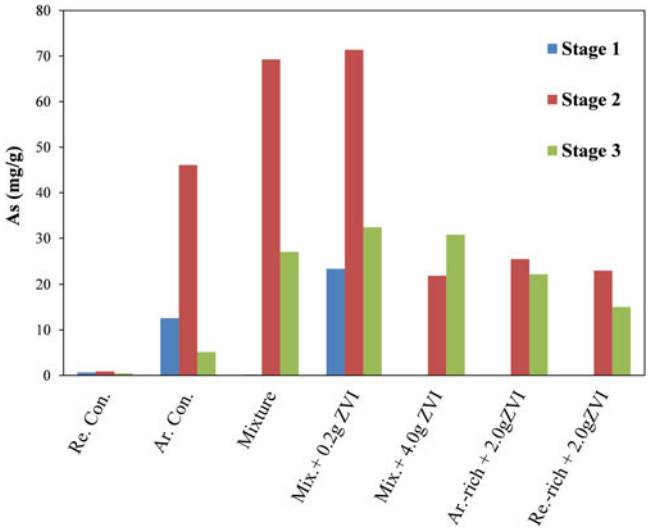


**Fig. 8.** Total arsenic quantity in amorphous iron precipitates.

## Environmental implications

Arsenic pollution in the Shimen realgar mine of Hunan originated from the mining of realgar and orpiment. Unfortunately, among the three thousand villagers of the region, more than one thousand have shown an average hair arsenic content of 0.972–2.459 μg/g indicative of poisoning (Wang *et al.*, 1999). Tailings containing realgar occur widely in mine areas and calcining zones (Fig. 9*a*), and remediation of arsenic-containing realgar tailings is needed urgently. Arsenic-containing tailings amounting to ~$2.7\times10^5$ t (including soil and settlement tailings) will be disposed to landfill areas according to current estimation. The previous study by the present authors showed that realgar and related settlement tailings will produce acid, and ZVI addition can potentially remediate arsenic release from Fe-deficient arsenic-containing tailings (Fan *et al.*, 2018a,b). The present study has shown that mixing two different kinds of arsenic-containing tailings does not aggravate but actually reduces both arsenic release and acid mine drainage. This finding will help in the centralised treatment of arsenic pollution in polymetallic mine areas due to the variety of tailings and limited land. At the time of writing, the comprehensive treatment of arsenic-containing tailings is underway in the Shimen mine (Fig. 9*b*). The current finding may inspire the processing of tailings in similar mine areas.

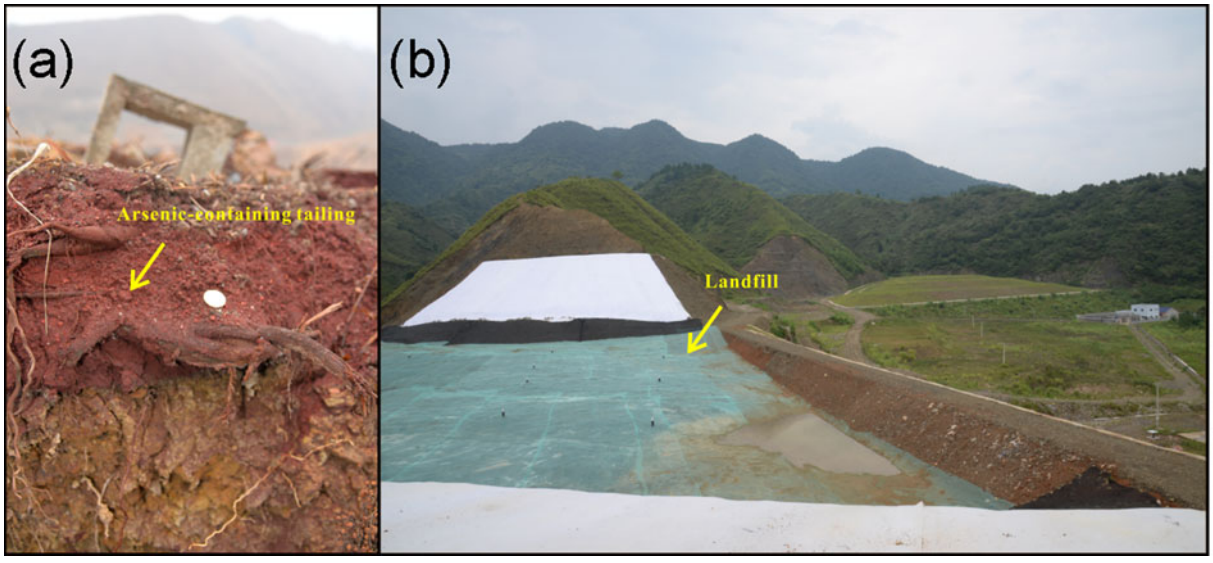


**Fig. 9.** Arsenic-containing tailings from the Shimen realgar mine (*a*) and construction of the proposed landfill (*b*). The coin in (*a*) is 2 cm in diameter.

https://doi.org/10.1180/mgm.2020.26 Published online by Cambridge University Press

## Conclusions

The possibility of mixing two typical arsenic-containing tailings to reduce arsenic release and control acid generation was discussed here, and the subject of whether exogenous ZVI can restrain arsenic release also, was investigated. The major findings are summarised as follows:

(1) The dissolution of arsenopyrite by *Acidithiobacillus ferrooxidans* results in decreased solution pH. Mixing the two tested tailings initially increased pH and reduced arsenic release due to pH control and decreasing $Fe^{3+}$. These trends were obvious for the tailings mixture in Stages 1 and 2.
(2) A small amount of ZVI (0.2 g) limited arsenic release from the tailings mixture effectively, and a much larger amount of ZVI (4.0 g) further reduced arsenic release to 0.003 mg/g, a level lower than that of the control groups. An intermediate amount of ZVI (2.0 g) can be applied along with additional realgar tailings in the tailings mixture to jointly restrict arsenic release.
(3) ATR–FTIR spectra confirmed that mixed tailings reduced arsenic dissolution by *A. ferrooxidans* and accounted for the decrease in arsenic release. When ZVI was added, the attenuation of arsenic release could additionally benefit from the adsorption and uptake of As(V) and As(III) by secondary Fe–As(III) and Fe–As(V) precipitates and by Fe–As(V) crystalline phases. Smaller amounts of arsenic were found in the amorphous Fe precipitate in the 4.0 g ZVI group (0.006 mg/g in Stage 1, 21.90 mg/g in Stage 2 and 30.75 mg/g in Stage 3) compared with those of the 0.2 g ZVI group (23.28 mg/g in Stage 1, 71.39 mg/g in Stage 2 and 32.38 mg/g in Stage 3). Release of arsenic by the 4.0 g ZVI group increased obviously in Stage 3 only.
(4) A low-cost and integrated strategy for treating arsenic-containing tailings would be to mix two typical tailings and add exogenous slag ZVI.

**Acknowledgements.** The present study was supported by the National Natural Science Foundation of China (No. 41772367).

**Supplementary material.** To view supplementary material for this article, please visit https://doi.org/10.1180/mgm.2020.26

## References

Bao Z. (1991) A discussion on gold potential of pyrite and arsenopyrite in gold-bearing deposit, Hunan Province (in Chinese). *Mineral Resources & Geology*, **5**, 368–374.

Baragaño D., Alonso J., Gallego J., Lobo M. and Gil-Díaz M. (2020) Zero valent iron and goethite nanoparticles as new promising remediation techniques for As-polluted soils. *Chemosphere*, **238**, 124624.

Bertocchi A.F., Ghiani M., Peretti R. and Zucca A. (2006) Red mud and fly ash for remediation of mine sites contaminated with As, Cd, Cu, Pb and Zn. *Journal of Hazardous Materials*, **134**, 112–119.

Bluteau M.C. and Demopoulos G.P. (2007) The incongruent dissolution of scorodite — solubility, kinetics and mechanism. *Hydrometallurgy*, **87**, 163–177.

Bowell R., Alpers C., Jamieson H., Nordstrom K. and Majzlan J. (2014) *Arsenic: Environmental Geochemistry, Mineralogy, and Microbiology*. Walter de Gruyter GmbH & Co KG, Berlin.

Carlson L., Bigham J.M., Schwertmann U., Kyek A. and Wagner F. (2002) Scavenging of As from acid mine drainage by schwertmannite and ferrihydrite: A comparison with synthetic analogues. *Environmental Science & Technology*, **36**, 1712–1719.

Chang-Li M.O., Feng-Chang W.U., Zhi-You F.U., Zhu J. and Ran L. (2013) Antimony, arsenic and mercury pollution in agricultural soil of antimony mine area in Xikuangshan, Hunan. *Acta Mineralogica Sinica*, **33**, 344–350.

Chowdhury T.R., Mandal B.K., Samanta G., Basu G.K., Chowdhury P.P., Chanda C.R., Karan N.K., Lodh D., Dhar R.K. and Das D. (1997) Arsenic in groundwater in six districts of West Bengal, India: The biggest arsenic calamity in the world: The status report up to August, 1995. Pp. 93–111 in: *Arsenic* (C.O. Abernathy, R.L. Calderon and W.R. Chappell, editors). Springer, Dordrecht, The Netherlands.

Corkhill C.L. and Vaughan D.J. (2009) Arsenopyrite oxidation – a review. *Applied Geochemistry*, **24**, 2342–2361.

Deng Sha Gu Guohua Xu Baoke Li Lijuan Wu and Bichao. (2018) Surface characterization of arsenopyrite during chemical and biological oxidation. *Science of the Total Environment*, **626**, 349–356.

Dermatas D., Moon D.H., Menounou N. and Xiaoguang Meng R.H. (2004) An evaluation of arsenic release from monolithic solids using a modified semi-dynamic leaching test. *Journal of Hazardous Materials*, **116**, 25–38.

Drahota P., Mihaljevič M., Grygar T., Rohovec J. and Pertold Z. (2011) Seasonal variations of Zn, Cu, As and Mo in arsenic-rich stream at the Mokrsko gold deposit, Czech Republic. *Environmental Earth Sciences*, **62**, 429–441.

Fan L., Zhao F., Liu J. and Frost R.L. (2018a) The As behavior of natural arsenical-containing colloidal ferric oxyhydroxide reacted with sulfate reducing bacteria. *Chemical Engineering Journal*, **332**, 183–191.

Fan L., Zhao F., Liu J. and Hudson-Edwards K.A. (2018b) Dissolution of realgar by *Acidithiobacillus ferrooxidans* in the presence and absence of zerovalent iron: Implications for remediation of iron-deficient realgar tailings. *Chemosphere*, **209**, 381–391.

Gil-Díaz M., Rodríguez-Valdés E., Alonso J., Baragaño D., Gallego J.R. and Lobo M.C. (2019) Nanoremediation and long-term monitoring of brownfield soil highly polluted with As and Hg. *Science of The Total Environment*, **675**, 165–175.

Goldberg S. and Johnston C.T. (2001) Mechanisms of arsenic adsorption on amorphous oxides evaluated using macroscopic measurements, vibrational spectroscopy, and surface complexation modeling. *Journal of Colloid and Interface Science*, **234**, 204–216.

Goossens D., Buck B.J., Teng Y. and Mclaurin B.T. (2015) Surface and airborne arsenic concentrations in a recreational site near Las Vegas, Nevada, USA. *PLOS One*, **10**, e0124271.

Gruyter W.D. (2014) Arsenic: Environmental geochemistry, mineralogy, and microbiology. *BMJ*, **1**, 740–742.

He H., Cao J. and Duan N. (2019) Defects and their behaviors in mineral dissolution under water environment: A review. *Science of the Total Environment*, **651**, 2208–2217.

Henao D.M.O. and Godoy M.A.M. (2010) Jarosite pseudomorph formation from arsenopyrite oxidation using *Acidithiobacillus ferrooxidans*. *Hydrometallurgy*, **104**, 162–168.

Henke K. (2009) *Arsenic: Environmental Chemistry, Health Threats and Waste Treatment*. John Wiley & Sons, Hoboken, New Jersey, USA.

Hudson-Edwards K.A. (2016) Tackling mine wastes. *Science*, **352**, 288–290.

Hui Z., Ma D. and Hu X. (2002) Arsenic pollution in groundwater from Hetao Area, China. *Environmental Geology*, **41**, 638–643.

Kim K.R., Lee B.-T. and Kim K.-W. (2012) Arsenic stabilization in mine tailings using nano-sized magnetite and zero valent iron with the enhancement of mobility by surface coating. *Journal of Geochemical Exploration*, **113**, 124–129.

Ladeira A.C. and Ciminelli V.S. (2004) Adsorption and desorption of arsenic on an oxisol and its constituents. *Water Research*, **38**, 2087–2094.

Langmuir D., Mahoney J. and Rowson J. (2006) Solubility products of amorphous ferric arsenate and crystalline scorodite ($FeAsO_4{\cdot}2H_2O$) and their application to arsenic behavior in buried mine tailings. *Geochimica et Cosmochimica Acta*, **70**, 2942–2956.

Lengke M.F. and Tempel R.N. (2003) Natural realgar and amorphous AsS oxidation kinetics. *Geochimica et Cosmochimica Acta*, **67**, 859–871.

Lingmei W., Chaoyang W., Linsheng Y. (2009) Using rice as bio-indicator for heavy metal contamination, a study in the Pb–Zn mining and smelting area

at Shuikoushan, Hunan Province, China. *Asian Journal of Ecotoxicology*, **4**, 373–381 [in Chinese].

Liu F., Zhang W., Tao L., Hao B. and Zhang J. (2019) Simultaneously photocatalytic redox and removal of chromium(VI) and arsenic(III) by hydrothermal carbon-sphere@nano-$Fe_3O_4$. *Environmental Science: Nano*, **6**, 937–947.

Liu J., Cheng H., Zhao F., Dong F. and Frost R.L. (2013) Effect of reactive bed mineralogy on arsenic retention and permeability of synthetic arsenic-containing acid mine drainage. *Journal of Colloid & Interface Science*, **394**, 530–538.

Liu J., Deng S., Zhao F., Cheng H. and Frost R.L. (2014) Spectroscopic characterization and solubility investigation on the effects of As(V) on mineral structure tooeleite ($Fe_6(AsO_3)_2SO_4(OH)_2{\cdot}H_2O$). *Spectrochimica Acta Part A: Molecular and Biomolecular Spectrosccopy,* **134C**, 428–433.

Liu J., He L., Chen S., Dong F. and Frost R.L. (2016) Characterization of the dissolution of tooeleite under *Acidithiobacillus ferrooxidans* relevant to mineral trap for arsenic removal. *Desalination and Water Treatment*, **57**, 15108–15114.

Liu J., He L., Dong F. and Frost R.L. (2017a) Infrared and Raman spectroscopic characterizations on new Fe sulphoarsenate hilarionite ($Fe_2((III))(SO_4)(AsO_4)(OH){\cdot}6H_2O$): Implications for arsenic mineralogy in supergene environment of mine area. *Spectrochimica Acta Part A: Molecular and Biomolecular Spectrosccopy*, **170**, 9–13.

Liu J., Zhou L., Dong F. and Hudson-Edwards K.A. (2017b) Enhancing As(V) adsorption and passivation using biologically formed nano-sized FeS coatings on limestone: Implications for acid mine drainage treatment and neutralization. *Chemosphere*, **168**, 529–538.

Liu Y.J., Gan Y.Q., Wang Y.X., Ma T. and Li J.L. (2010) An experimental study on removing arsenic from water using iron slag. *Environmental Science & Technology*, **33**, 166–170 [in Chinese].

Lockwood C.L., Mortimer R.J.G., Stewart D.I., Mayes W.M., Peacock C.L., Polya D.A., Lythgoe P.R., Lehoux A.P., Gruiz K. and Burke I.T. (2014) Mobilisation of arsenic from bauxite residue (red mud) affected soils: Effect of pH and redox conditions. *Applied Geochemistry*, **51**, 268–277.

Loehr T.M. and Plane R.A. (1968) Raman spectra and structures of arsenious acid and arsenites in aqueous solution. *Inorganic Chemistry*, **7**, 1708–1714.

Lottermoser B. (2007) *Mine Wastes* (second edition): *Characterization, Treatment, Environmental Impacts*. Springer, Berline, 304 pp.

Mohapatra M., Sahoo S.K., Anand S. and Das R.P. (2006) Removal of As(V) by Cu(II)-, Ni(II)-, or Co(II)-doped goethite samples. *Journal of Colloid & Interface Science*, **298**, 6–12.

Nesbitt H.W. and Muir I.J. (1998) Oxidation states and speciation of secondary products on pyrite and arsenopyrite reacted with mine waste waters and air. *Mineralogy & Petrology*, **62**, 123–144.

Ouyang B., Lu X., Liu H., Li J., Zhu T., Zhu X., Lu J. and Wang R. (2014) Reduction of jarosite by *Shewanella oneidensis* MR-1 and secondary mineralization. *Geochimica et Cosmochimica Acta*, **124**, 54–71.

Pu W. (1950) The geology of Sn-As ore in Anyuan area of Bing country, Hunan Province, China. *Geological Review*, **6**, 176 [in Chinese].

Qiao J.T., Liu T.X., Wang X.Q., Li F.B., Lv Y.H., Cui J.H., Zeng X.D., Yuan Y.Z. and Liu C.P. (2017) Simultaneous alleviation of cadmium and arsenic accumulation in rice by applying zero-valent iron and biochar to contaminated paddy soils. *Chemosphere*, **195**, 260–271.

Rodríguez-Lado L., Sun G., Berg M., Zhang Q., Xue H., Zheng Q. and Johnson C.A. (2013) Groundwater arsenic contamination throughout China. *Science*, **341**, 866–868.

Schwertmann U. and Cornell R.M. (1993) Iron oxides in laboratory. *Soil Science*, **156**, 281–282.

Shelobolina E.S., Avakyan Z.A. and Karavaiko G.I. (1999) *Transformation of Iron-Containing Minerals in Kaolin During Growth of a Mixed Bacterial Culture Derived from Kaolin*. Springer, Berlin.

Shrestha R.R., Shrestha M.P., Upadhyay N.P., Pradhan R., Khadka R., Maskey A., Maharjan M., Tuladhar S., Dahal B.M. and Shrestha K. (2003) Groundwater arsenic contamination, its health impact and mitigation program in Nepal. *Journal of Environmental Science and Health Part A: Toxic/Hazardous Substances and Environmental Engineering*, **38**, 185–200.

Silverman M.P. and Lundgren D.G. (1959) Studies on the chemoautotrophic iron bacterium *Ferrobacillus ferrooxidans*: I. An improved medium and a harvesting procedure for securing high cell yields. *Journal of Bacteriology*, **77**, 642–647.

Singer P.C. and Stumm W. (1970) Acidic mine drainage: The rate-determining step. *Science*, **167**, 1121.

Šlejkovec Z., Elteren J.T.v., Glass H.-J., Jeran Z. and Jaćimović R. (2010) Speciation analysis to unravel the soil-to-plant transfer in highly arsenic-contaminated areas in Cornwall (UK). *International Journal of Environmental Analytical Chemistry*, **90**, 784–796.

Smedley P.L and Kinniburgh and D.G. (2002) A review of the source, behaviour and distribution of arsenic in natural waters. *Applied Geochemistry*, **17**, 517–568.

Su H., Fang Z., Tsang P.E., Fang J. and Zhao D. (2016) Stabilisation of nanoscale zero-valent iron with biochar for enhanced transport and in-situ remediation of hexavalent chromium in soil. *Environmental Pollution*, **214**, 94–100.

Tang J., Liao Y., Yang Z., Chai L. and Yang W. (2016) Characterization of arsenic serious-contaminated soils from Shimen realgar mine area, the Asian largest realgar deposit in China. *Journal of Soils & Sediments*, **16**, 1519–1528.

Teixeira M.C. and Ciminelli V.S. (2005) Development of a biosorbent for arsenite: Structural modeling based on X-ray spectroscopy. *Environmental Science & Technology*, **39**, 895–900.

Tossell J.A. (1997) Theoretical studies on arsenic oxide and hydroxide species in minerals and in aqueous solution. *Geochimica et Cosmochimica Acta*, **61**, 1613–1623.

Vítková M., Puschenreiter M. and Komárek M. (2018) Effect of nano zero-valent iron application on As, Cd, Pb, and Zn availability in the rhizosphere of metal(loid) contaminated soils. *Chemosphere*, **200**, 217–226.

Van Den Berghe M.D., Jamieson H.E. and Palmer M.J. (2018) Arsenic mobility and characterization in lakes impacted by gold ore roasting, Yellowknife, NWT, Canada. *Environmental Pollution*, **234**, 630–641.

Wang Y. and Reardon E.J. (2001) A siderite/limestone reactor to remove arsenic and cadmium from wastewaters. *Applied Geochemistry*, **16**, 1241–1249.

Wang Z., He H., Yan Y. and Wu C. (1999) Arsenic exposure of residents in areas near Shimen arsenic mine. *Journal of Hygiene Research*, **28**, 12–14.

Xiang B.Z., Jiang W.R. and Min B.J. (2000) Typomorphic characteristics of arsenopyrite in precambrian gold deposit, Hunan. *Gold Geology*, **6**, 39–45.

Zhu X., Wang R., Lu X., Liu H., Li J., Ouyang B. and Lu J. and Xiancai. (2015) Secondary minerals of weathered orpiment-realgar-bearing tailings in Shimen Carbonate-Type Realgar Mine, Changde, central China. *Mineralogy and Petrology*, **109**, 1–15.

https://doi.org/10.1180/mgm.2020.26 Published online by Cambridge University Press